Supporting Information

"The golden method": electrochemical is an efficient route to gold complexes

Luis M. González-Barcia, María J. Romero Ana M. González Noya, Manuel R. Bermejo, Marcelino Maneiro, Guillermo Zaragoza and Rosa Pedrido**

Experimental Section

Materials

All solvents, 2-(diphenylphosphino)benzaldehyde, 4-methoxyphenyl isothiocyanate, 4-nitrophenyl-3-thiosemicarbazide, hydrazine monohydrate, gold plate, gold(III) chloride hydrate, and 2,2′-thiodiethanol are commercially available and were used without further purification.

Physical Measurements

Elemental analysis of C, H, N and S were performed on a FISONS EA 1108 analyzer. ^{1}H NMR spectra were recorded on a Varian Mercury 300 spectrometer; ^{13}C and ^{31}P NMR spectra (H_3PO_4 was used as internal reference) were recorded on a Bruker DRX-500 MHz spectrometer. DMSO-d_6 was employed as deuterated solvent and chemical shifts were expressed relative to tetramethylsilane. Infrared spectra were measured from KBr pellets on a BRUKER IFS-66V spectrophotometer in the ranges 4000-100 or 500-100 cm^{-1}. Electrospray ionization mass spectra (ESI^+) were recorded on an API4000 Applied Biosystems mass spectrometer with Triple Cuadrupole analyser.

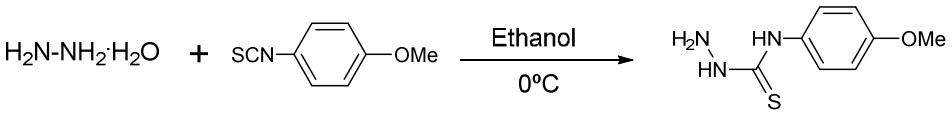

Scheme S1. Synthesis of the 4-methoxyphenylthiosemicarbazide

Synthesis of 4-methoxyphenylthiosemicarbazide

Hydrazine monohydrate (1.52 g, 30 mmol) was slowly added to a solution of 4-methoxyphenyl-isothiocyanate (2.47 g, 15 mmol) in absolute ethanol (20 mL) with stirring at 0 °C (ice bath). After 1 hour the white solid was filtered off, washed with ethanol and diethyl ether and dried under vacuum.

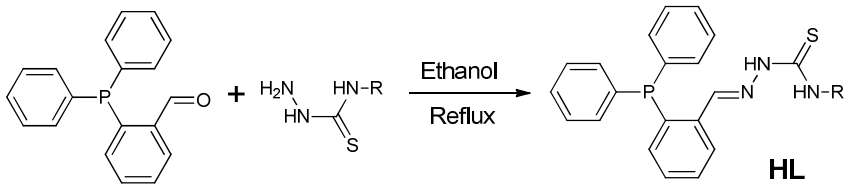

Scheme S2. Synthesis of the ligands HL^n (HL^1, R = Me; HL^2, R =Et; HL^3, R = Ph; HL^4, R = PhOMe; HL^5, R = $PhNO_2$)

Synthesis of the ligands HL^n
(HL^1, R = Me; HL^2, R = Et; HL^3, R = Ph; HL^4, R = PhOMe; HL^5, R = $PhNO_2$)

All ligands were synthesised following the same procedure. We must point out herein that HL^1, HL^2 and HL^3 were previously reported.[1-3] For that reason we have included here the experimental data for HL^{4-5} only. As an example, we can see below the synthesis of HL^4.

The ligand 4-methoxyphenylthiosemicarbazone, HL^4, was prepared by condensation of 2-diphenylphosphinobenzaldehyde (1.0 g, 3.4 mmol) with 4-methoxyphenyl-thiosemicarbazide (0.7 g, 3.4 mmol) in absolute ethanol (25 mL). The solution was heated under reflux for 4 h and concentrated with a Dean–Stark trap. The yellow precipitate was collected by filtration. The resulting solid was finally washed with diethyl ether (3 × 10 mL) and dried *in vacuo.*

HL^4. Yellow solid. Yield 1.076 g (67 %); m.p.= 161-163 ºC; E.A. (Found: C, 68.8; H, 5.3; N, 8.9;S, 6.6; $C_{27}H_{24}N_3OPS$ required: C, 69.1; H, 5.2; N, 8.9; S, 6.8); ESI^+ MS (m/z) 470.1 $[HL + H]^+$; ^1H NMR (300 MHz, DMSO-d_6, ppm): δ 11.86 (s, $1H_a$), 9.77 (s, $1H_b$), 8.75 (d, J= 4.7 Hz, $1H_c$), 8.30 (dd, J_1= 7.5 Hz, J_2= 3.7 Hz, $1H_d$), 7.34-7.49 (m, 11H), 7.12-7.26 (m, 4H), 6.91 (d, J = 8.7 Hz, 1H), 6.79 (dd, J_1 = 6.6 Hz, J_2= 4.8 Hz, 1H), 3.75 (s, 3H); ^{13}C NMR (126 MHz, DMSO-d_6, ppm): δ 176.69 (C=S), 157.42 (C_{ar}-OCH_3) 141.22 (C=N), 137.95-127.92 (C_{ar}), 55.68 (O-CH_3); ^{31}P NMR (202 MHz, DMSO-d_6, ppm): δ -12.30; IR (KBr, cm^{-1}): ν(NH) 3229, 3155, ν(C=N) + ν(C-N) 1595, 1547, 1506, ν(C=S) 1090, 802, ν(N-N) 1037.

HL^5. Yellow solid. Yield 1.498 g (92%); m.p.= 240-242 ºC; E.A. (Found: C, 64.3; H, 4.6; N, 11.4; S, 6.3; $C_{26}H_{21}N_4O_2PS$ required: C, 64.5; H, 4.4; N, 11.6; S, 6.6; ESI^- MS (m/z) 483.1 $[L]^-$; 499.1 $[L + O]^-$; ^1H NMR (500 MHz, DMSO-d_6, ppm): δ 12.30 (s, $1H_a$), 10.33 (s, $1H_b$), 8.88 (d, J= 4.9 Hz, $1H_c$), 8.35 (dd, J_1= 7.3 Hz, J_2= 4.1 Hz, $1H_d$), 8.24-7.21 (m, 16H), 6.81 (dd, J_1= 6.9 Hz, J_2= 4.4 Hz, 1H); ^{13}C NMR (126 MHz, DMSO-d_6, ppm): δ 175.24 (C=S), 144.89 (C=N), 143.14-123.42 (C_{ar}); ^{31}P NMR (202 MHz, DMSO-d_6, ppm): δ -12.76; IR (ATR, cm^{-1}): ν(NH) 3302, ν(NH) 3196, ν(C=N) + ν(C-N) 1597, 1539, 1514, $\nu(NO_2)$ 1333, ν(C=S) 1111, 851.

Electrochemical synthesis of gold(I) complexes

All syntheses were performed under the same experimental conditions: 0.1 g of ligand electrolysed at 5 mA (10.5-13.5 V) under argon atmosphere. As example we detail below the experimental procedure for the complex $[Au_2(L^1)_2]$.

Electrochemical synthesis of $[Au_2(L^1)_2]$

A suspension of the ligand HL^1 (0.1 g, 0.265 mmol) containing tetraethylammonium perchlorate as supporting electrolyte, a platinum wire as cathode and a gold plate as anode, was electrolysed in degassed acetonitrile (80 mL) for 85 min. The reaction was carried out at 5 mA (10.5 V) under argon atmosphere. The resulting yellow solution was concentrated under reduced pressure until half volume. Slow evaporation from the mother liquors afforded single crystals suitable for X-ray diffraction studies that were filtered, washed with diethyl ether and dried in vacuo, providing 0.093 g of a yellow crystalline product. The structure of this complex was found to be $[Au_2(L^1)_2]$ (**1**).

***Caution!** Perchlorate salts are potentially explosive and should be handled with care.

$[Au_2(L^1)_2]$. Yellow solid. Yield 0.093 g (61%); E.A. (Found: C, 44.0; N, 7.5; H, 3.2; S, 5.4; calculated for $Au_2C_{42}H_{38}N_6P_2S_2$: C, 43.9; N, 7.3; H: 3.3; S, 5.6; MALDI-TOF MS (m/z) 949.1 $[ML_2 + H]$, 1270.1 $[M_2L_2]\cdot 3CH_3CN$; ^{1}H NMR (300 MHz, DMSO-d_6, ppm): δ 8.21 (s, 1H, H_c), 7.72 (s, 1H), 7.57-7.33 (m, 13H_{Ar}), 7.02 (m, 1H, H_b), 2.75 (d, 3H, J= 4.6 Hz); ^{31}P NMR (202 MHz, DMSO-d_6, ppm): δ 33.7. IR (KBr, cm^{-1}): ν(OH) 3432, ν(C=N) + ν(C-N) 1540. 1461, 1436, ν(C=S) 1097, 791, ν(N-N) 1045.

$[Au_2(L^2)_2]\cdot 2H_2O$. Yellow solid. Yield 0.1 g (66%); E.A. (Found: C, 44.9; H, 3.8; N, 7.0; S, 5.3; calculated for $Au_2C_{44}H_{42}N_6P_2S_2$: C, 45.0; H, 3.6; N, 7.1; S, 5.4; MALDI-TOF MS (m/z) 588.1 [ML], 1175.0 $[M_2L_2]$, ^{1}H NMR (300 MHz, DMSO-d_6, ppm): 8.56 (s,1H, H_c), 8.32-6.11 (m, 14H_{Ar} + H_b) 3.27(q, 2H), 1.14 (t, 3H); ^{31}P NMR (202 MHz, DMSO-d_6, ppm): δ 33.9; IR (KBr, cm^{-1}): ν(NH) 3280, ν(C=N) + ν(C-N) 1479, 1457, 1434, ν(C=S) 1120, 800.

$[Au_2(L^3)_2]$. Yellow solid. Yield 0.084 g (60 %); E.A. (Found: C, 49.0; H, 3.5; N, 6.4; S, 4.8; calculated for $Au_2C_{52}H_{42}N_6P_2S_2$: C, 49.1; H, 3.3; N, 6.6; S, 5.0; ESI$^+$ MS (m/z) 636.1 $[ML + H]^+$, 1272.1 $[M_2L_2 + H]^+$, 1467.1; ^{1}H NMR (300 MHz, DMSO-d_6, ppm): δ 8.54 (s, 1H_c) 7.59-6.51 (m, 19H_{Ar} +H_b), ^{31}P NMR (202 MHz, DMSO-d_6, ppm): δ 39.7; IR (KBr, cm^{-1}): ν(NH) 3282, ν(C=N) + ν(C-N) 1481, 1463, 1410, ν(C=S) 1120, 796.

$[Au_2(L^4)_2]\cdot 2CH_3CN$. Yellow solid. Yield 0.080 g (58%); E.A. (Found: C, 48.9; N, 7.7; H, 3.7; S, 4.4; calculated for $Au_2C_{58}H_{52}N_8O_2P_2S_2$: C, 49.3; N, 7.9; H: 3.7; S, 4.5; ESI-FIA-TOF+ MS (m/z) 666.1 $[ML + H]^+$, 1331.0 $[M_2L_2 + H]^+$; ^{1}H NMR (300 MHz, DMSO-d_6, ppm): δ 9.00 (s, 1H, H_b), 8.04 (s, 1H, H_c), 7.77-6.58 (m, 18H), 3.66 (s, 3H); ^{31}P NMR (202 MHz, DMSO-d_6, ppm): δ 34.0.

IR (KBr, cm^{-1}): ν(OH) 3319, ν(C=N) + ν(C-N) 1510, 1479, 1437, ν(C=S) 1097, 795, ν(N-N) 1032. Slow evaporation from the mother liquors afforded yellow single crystals of $[Au_2(L^4)_2]\cdot 2CH_3CN$ (**2**$\cdot 2CH_3CN$) suitable for X-ray diffraction studies.

$[Au_2(L^5)_2]$. Yellow solid. Yield 0.071 g (51%); E.A. (Found: C, 45.7; H, 3.2; N, 8.2; S, 4.6; calculated for $Au_2C_{52}H_{40}N_8O_4P_2S_2$: C, 45.9; H, 3.0; N, 8.2; S, 4.7; MALDI-TOF MS (m/z) 682.2 [ML], 1360.1 [M_2L_2]; ^{1}H NMR (300 MHz, DMSO-d_6, ppm): δ 9.62 (s, 1H, H_b), 8.95 (s, 1H, H_c), 8.28-6.94 (m, 16H), 6.35 (dd,2H, J_1= 7.7 Hz J_2= 3.1 Hz); ^{31}P NMR (202 MHz, DMSO-d_6, ppm): δ 33.2, IR (KBr, cm^{-1}): ν(OH) 3402, ν(C=N) + ν(C-N) 1594, 1539 1495, ν(C=S) 1110, 804, ν(N-N) 1032

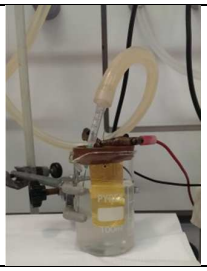	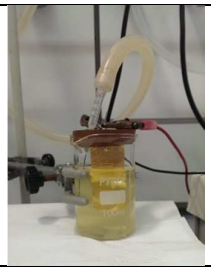
t= 0 min	t= 30 min
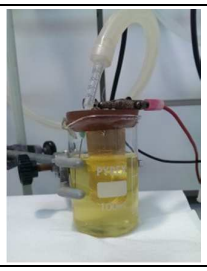	
t= 40 min	t= 68 min

Figure S1. Evolution of the electrochemical cell during the synthesis of $[Au_2(L^4)_2]\cdot 2CH_3CN$.

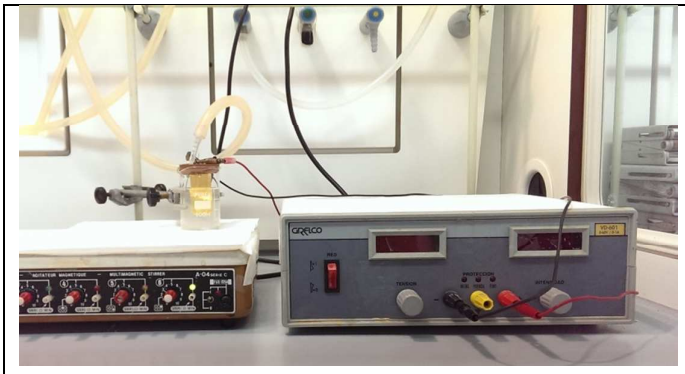	t= 0 min
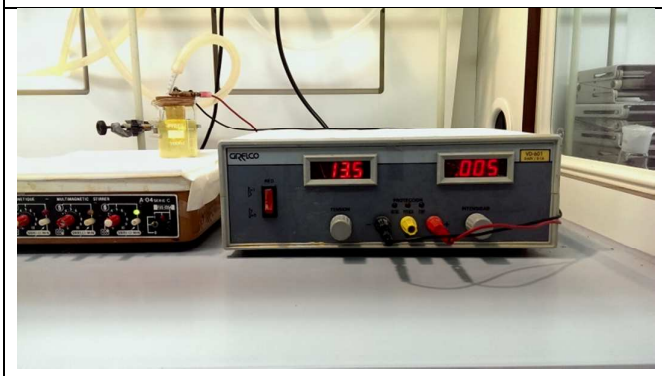	t= 30 min
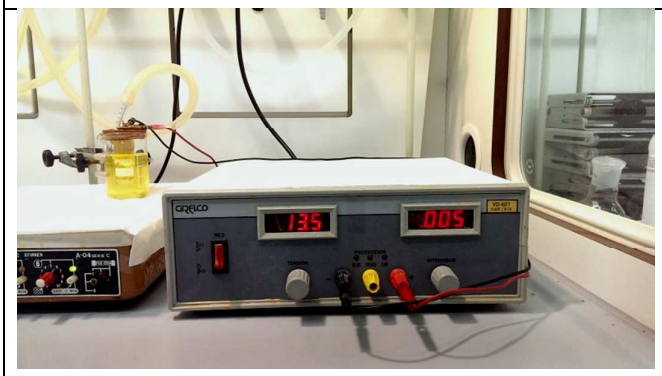	t= 40 min
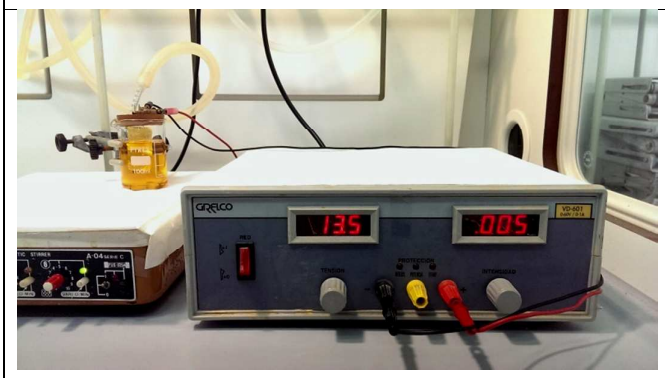	t= 68 min

Figure S2. Electrochemical parameters employed during the electrochemical synthesis of $[Au_2(L^4)_2]\cdot 2CH_3CN$.

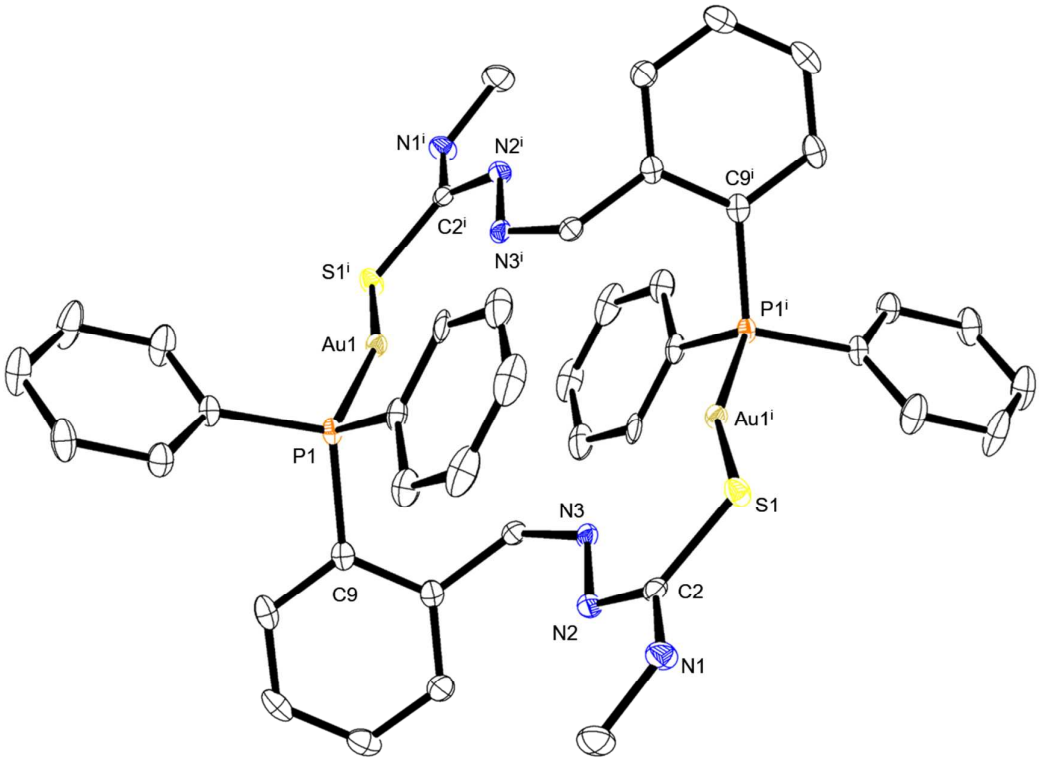

Figure S3. ORTEP depicture of the complex $[Au_2(L^1)_2]$. Hydrogen atoms have not been depicted for clarity.

Bond distances (Å)					
P1—Au1	2.2380 (7)	Au1—$S1^i$	2.3228 (7)	Au1-$N3^i$	2.523 (2)
Bond angles (º)					
P1—Au1—$S1^i$	158.79 (3)	C9—P1—Au1	115.05 (8)	Au1—$S1^i$—$C2^i$	103.68 (9)
Au1—$S1^i$—$N3^i$	75.54 (5)				

Table S1. Main bond distances [Å] and angles [º] for the complex $[Au_2(L^1)_2]$.

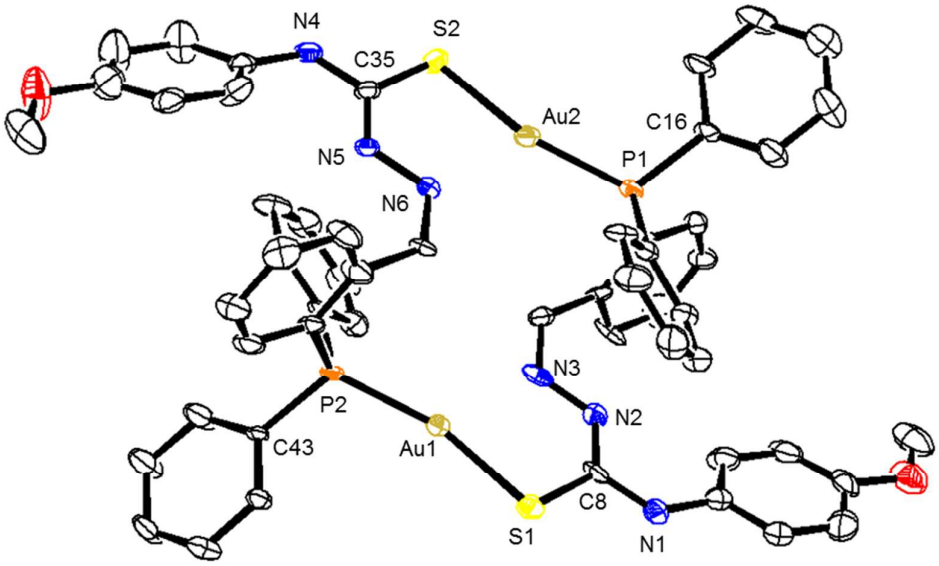

Figure S4. ORTEP depicture of the complex $[Au_2(L^4)_2]\cdot 2CH_3CN$. Hydrogen atoms and solvate acetonitrile molecules have not been depicted for clarity.

Bond distances (Å)					
N3—Au1	2.497 (7)	N6—Au2	2.474 (7)	P1—Au2	2.233 (3)
P2—Au1	2.226 (3)	S1—Au1	2.326 (3)	S2—Au2	2.337 (3)
Bond angles (º)					
P2—Au1—S1	164.29 (10)	C43—P2—Au1	115.3 (4)	C8—S1—Au1	102.5 (4)
P1—Au2—S2	162.66 (10)	C35—S2—Au2	102.0 (4)	C16—P1—Au2	113.6 (3)

Table S2. Main bond distances [Å] and angles [º] for the complex $[Au_2(L^4)_2]\cdot 2CH_3CN$.

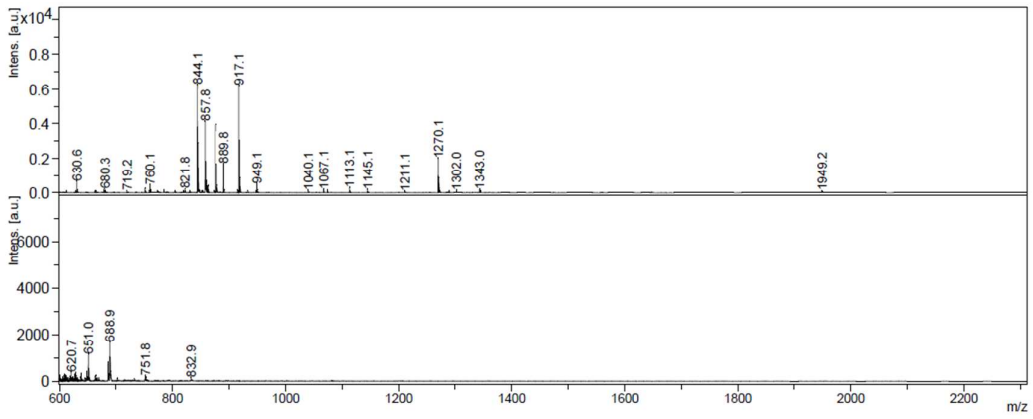

Figure S5. MALDI-TOF mass spectrum of $[Au_2(L^1)_2]$.

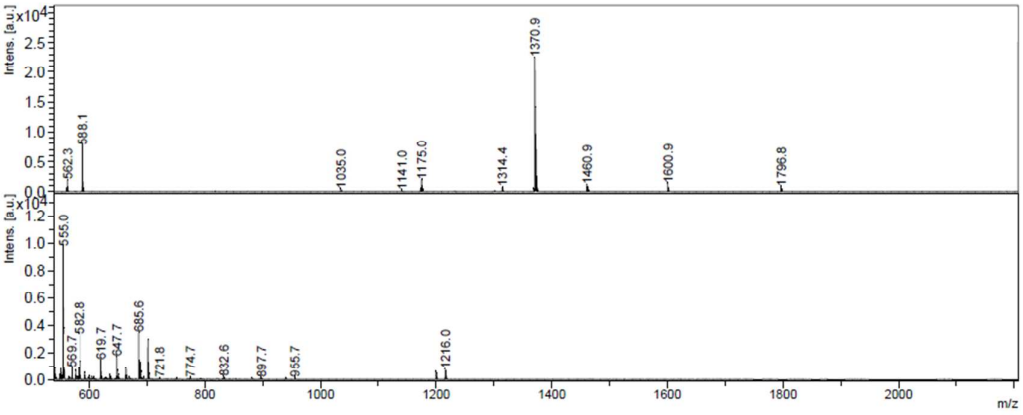

Figure S6. MALDI-TOF mass spectrum of $[Au_2(L^2)_2]\cdot 2H_2O$.

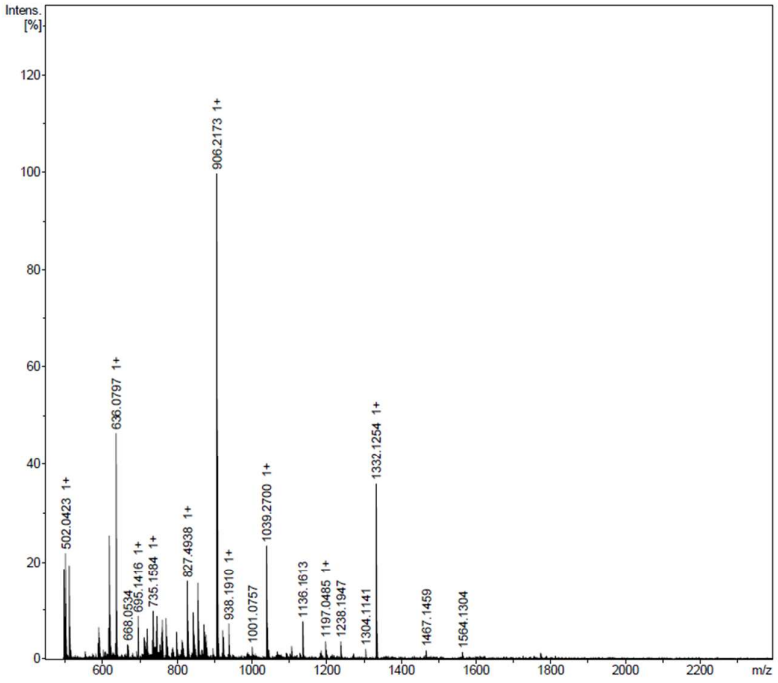

Figure S7. ESI$^+$ mass spectrum of $[Au_2(L^3)_2]$.

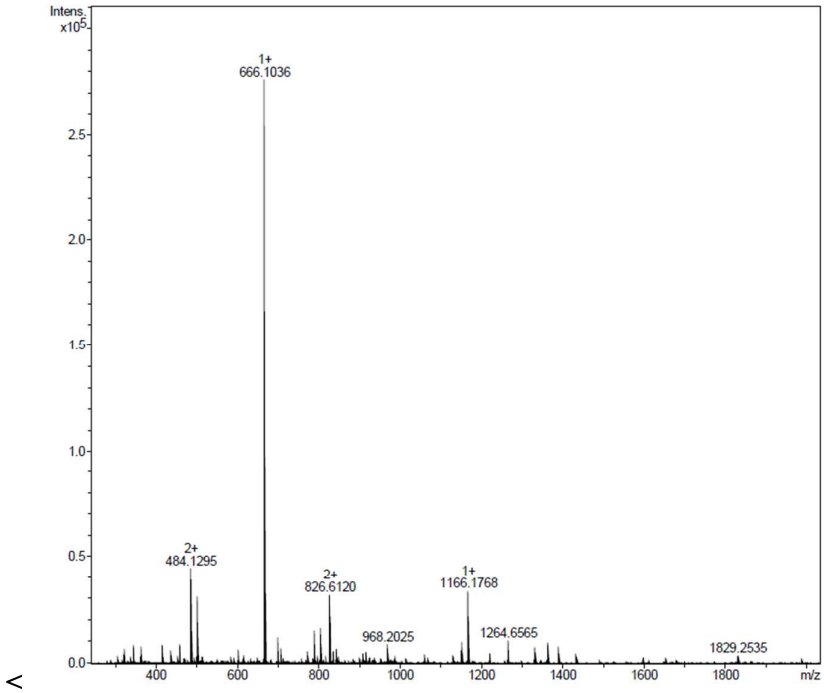

Figure S8. ESI-FIA-TOF$^+$ mass spectrum of $[Au_2(L^4)_2]\cdot 2CH_3CN$.

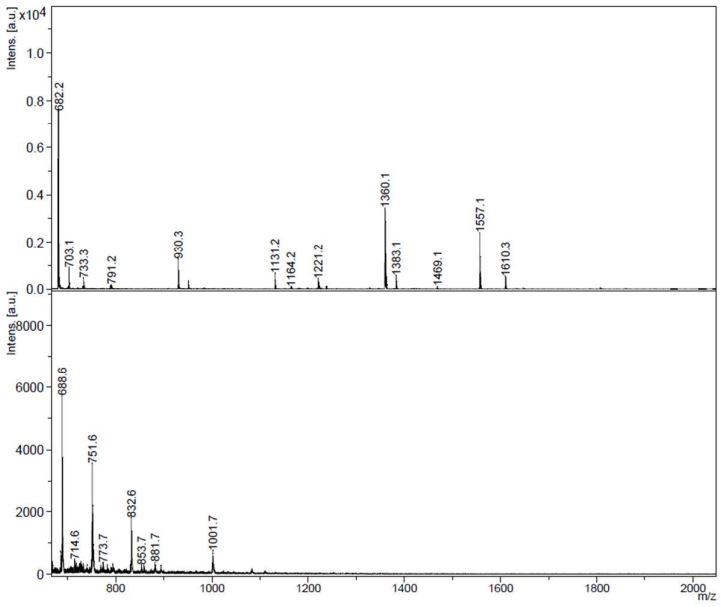

Figure S9. MALDI-TOF mass spectrum of $[Au_2(L^5)_2]$

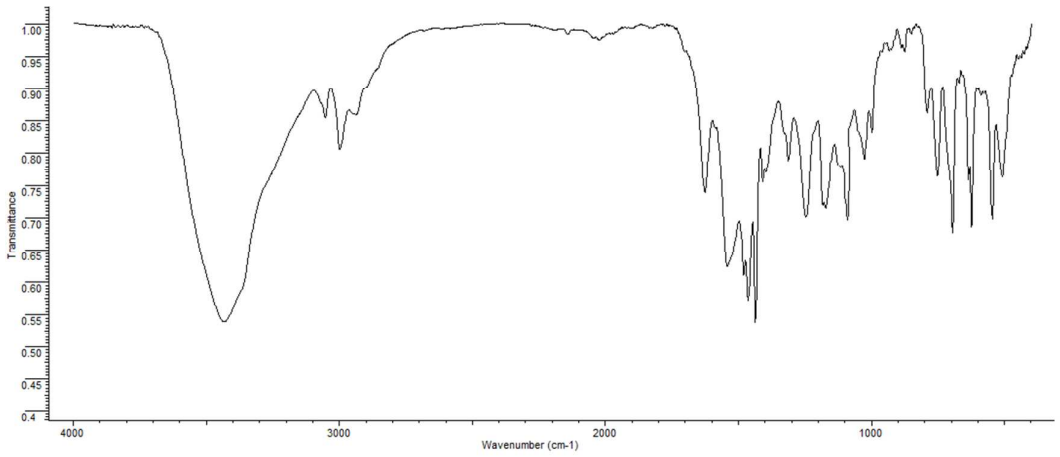

Figure S10. IR spectrum (cm^{-1}) of $[Au_2(L^1)_2]$.

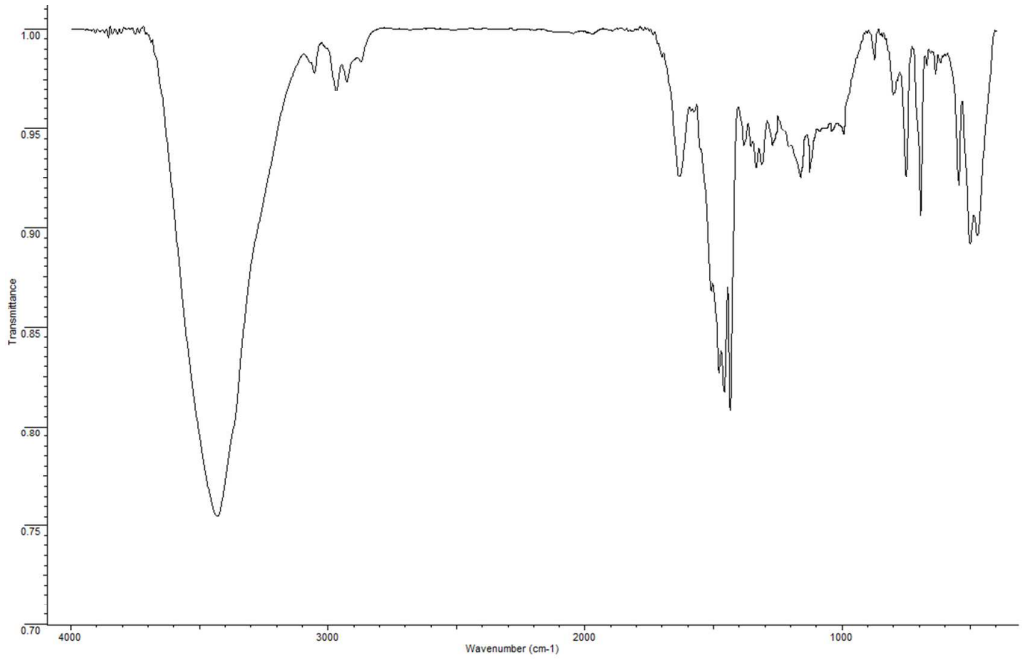

Figure S11. IR spectrum (cm^{-1}) of $[Au_2(L^2)_2]\cdot 2H_2O$.

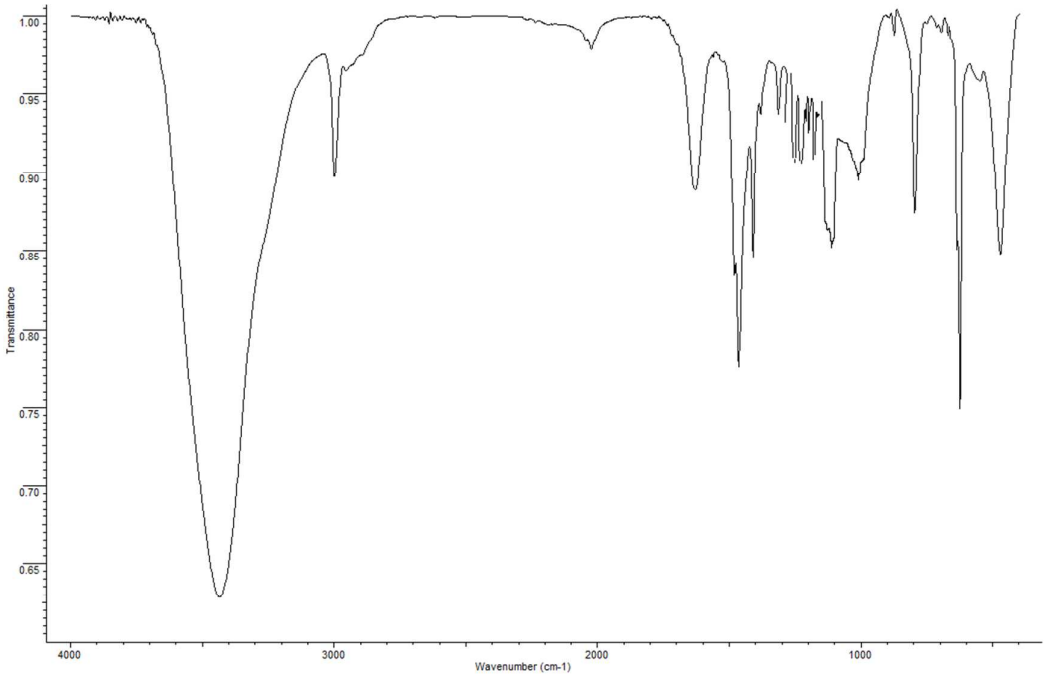

Figure S12. IR spectrum (cm^{-1}) of $[Au_2(L^3)_2]$.

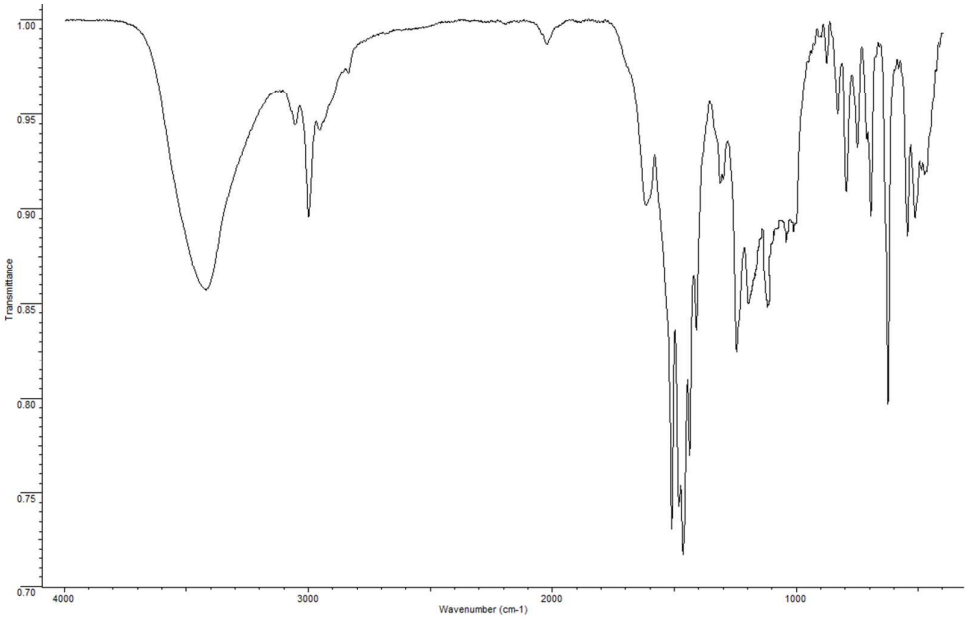

Figure S13. IR spectrum (cm^{-1}) of $[Au_2(L^4)_2]\cdot 2CH_3CN$.

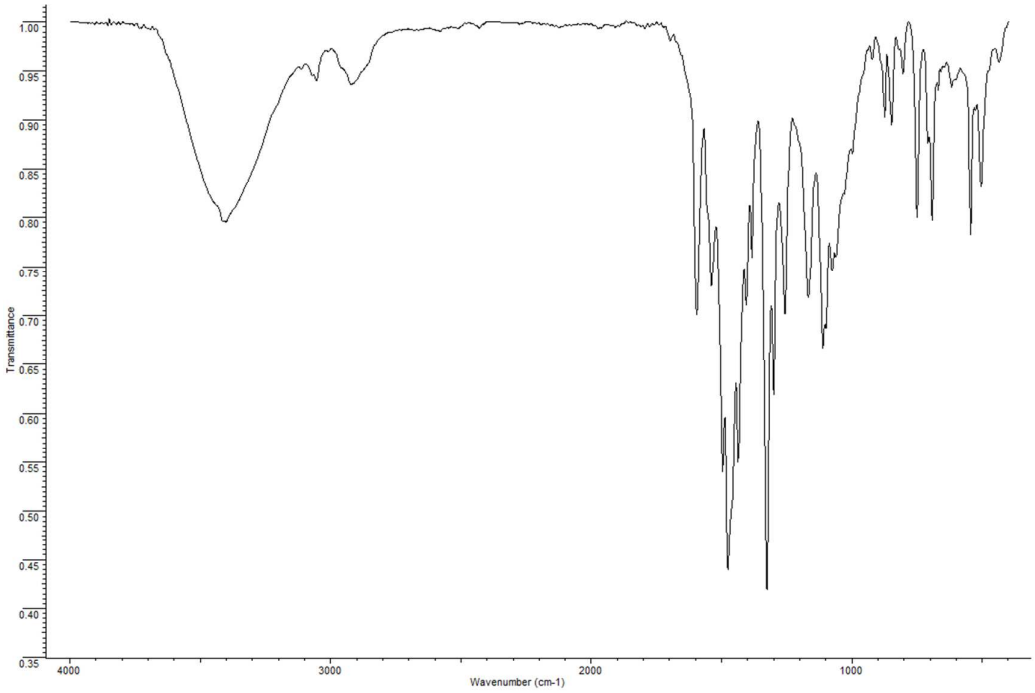

Figure S14. IR spectrum (cm^{-1}) of of $[Au_2(L^5)_2]$.

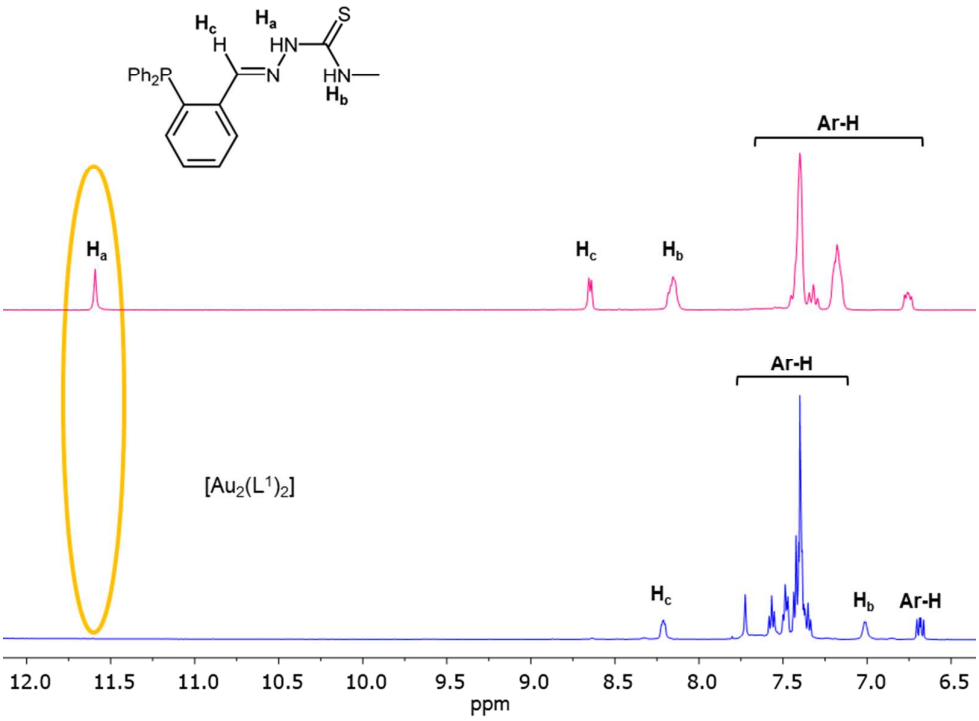

Figure S15. Overlapped ^{1}H NMR spectra of the ligand HL^{1} (top) and the complex $[Au_2(L^{1})_2]$ (bottom). Red ellipsoid stresses the disappearance of the NH proton in the complex obtained by electrochemical synthesis.

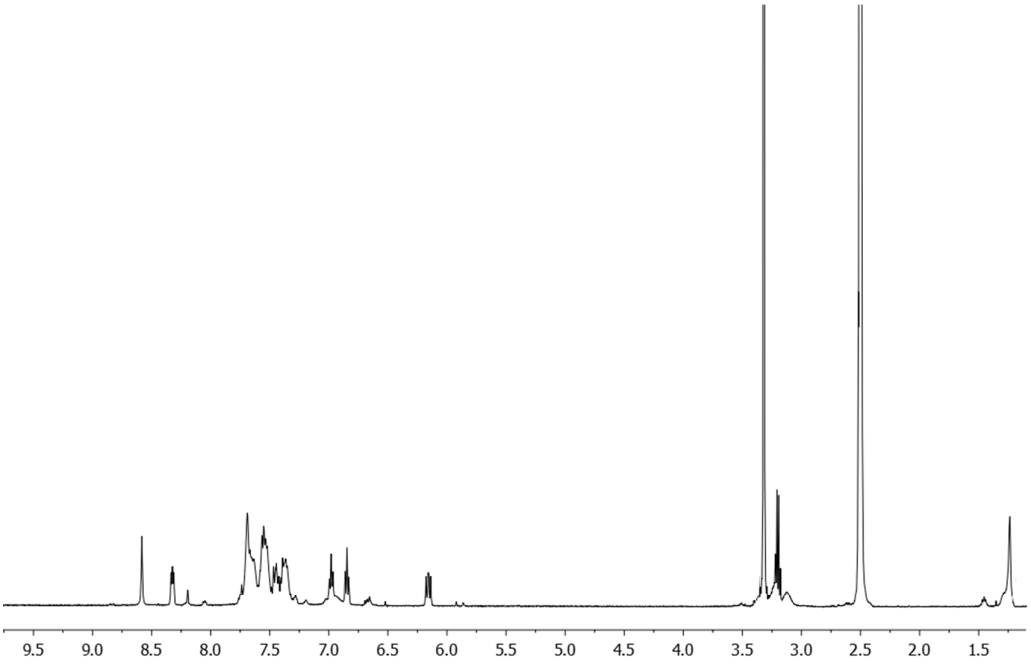

Figure S16. ^{1}H NMR spectrum of $[Au_2(L^{2})_2]\cdot 2H_2O$.

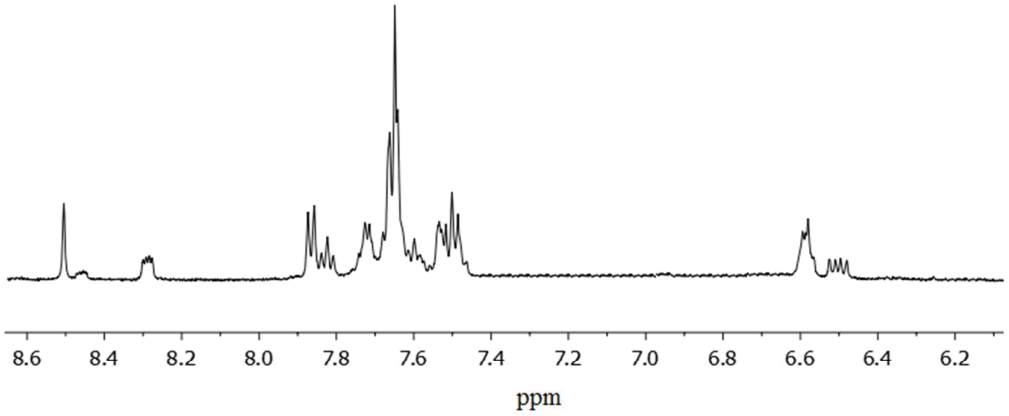

Figure S17. ^{1}H NMR spectrum of $[Au_2(L^3)_2]$.

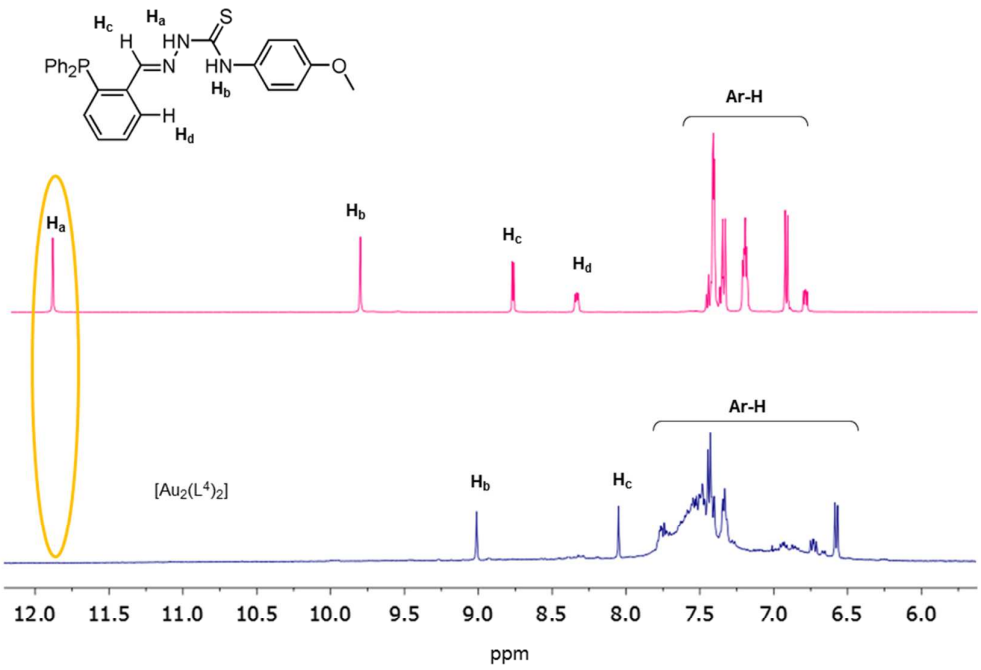

Figura S18. Overlapped ^{1}H NMR spectra of the ligand HL^4 (top) and the complex $[Au_2(L^4)_2]$ $2CH_3CN$ (bottom). Red ellipsoid stresses the disappearance of the NH proton in the complex obtained by electrochemical synthesis.

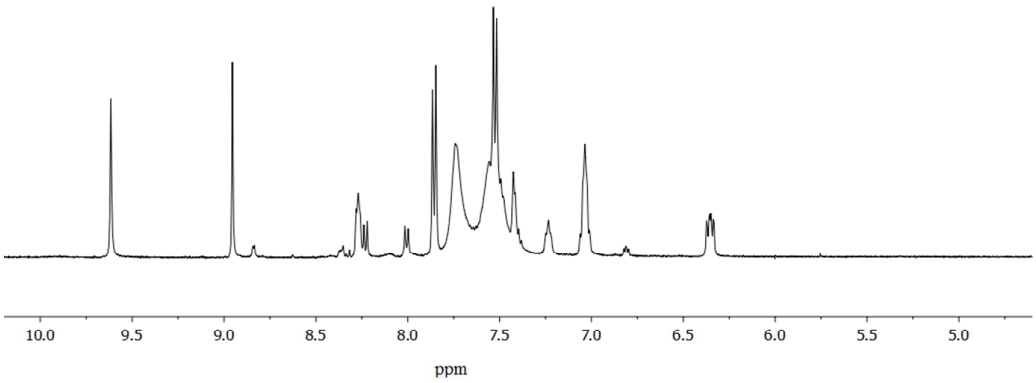

Figure S19. ^{1}H NMR spectrum of $[Au_2(L^5)_2]$.

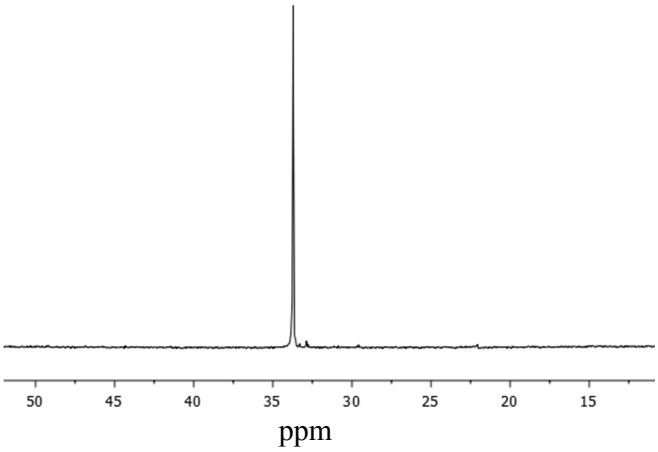

Figure S20. ^{31}P NMR spectrum of $[Au_2(L^1)_2]$.

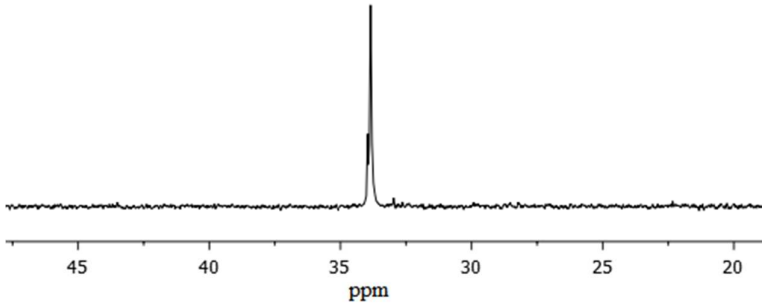

Figure S21. ^{31}P NMR spectrum of $[Au_2(L^2)_2]\cdot 2H_2O$.

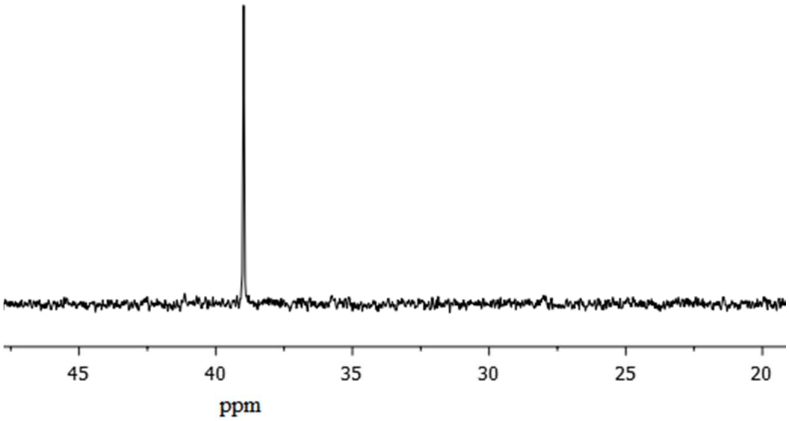

Figure S22. ^{31}P NMR spectrum of $[Au_2(L^3)_2]$.

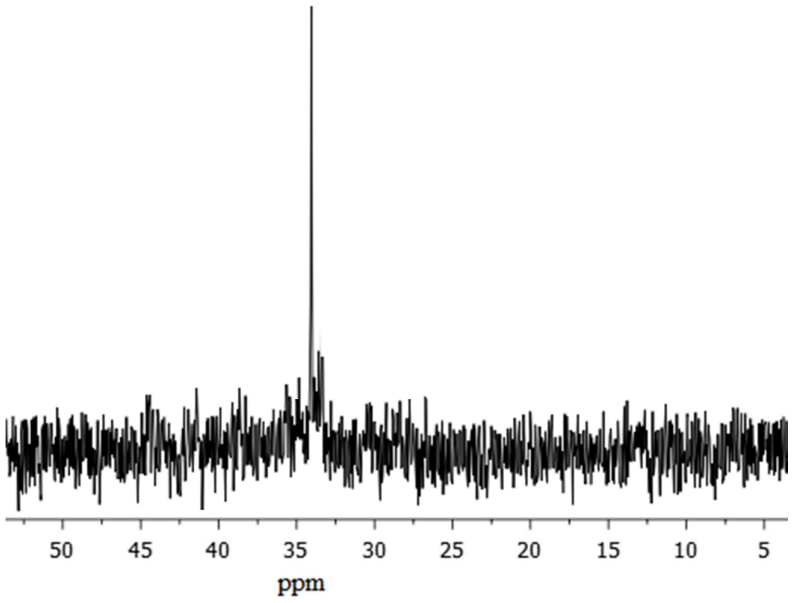

Figure S23. ^{31}P NMR spectrum of $[Au_2(L^4)_2]\cdot 2CH_3CN$.

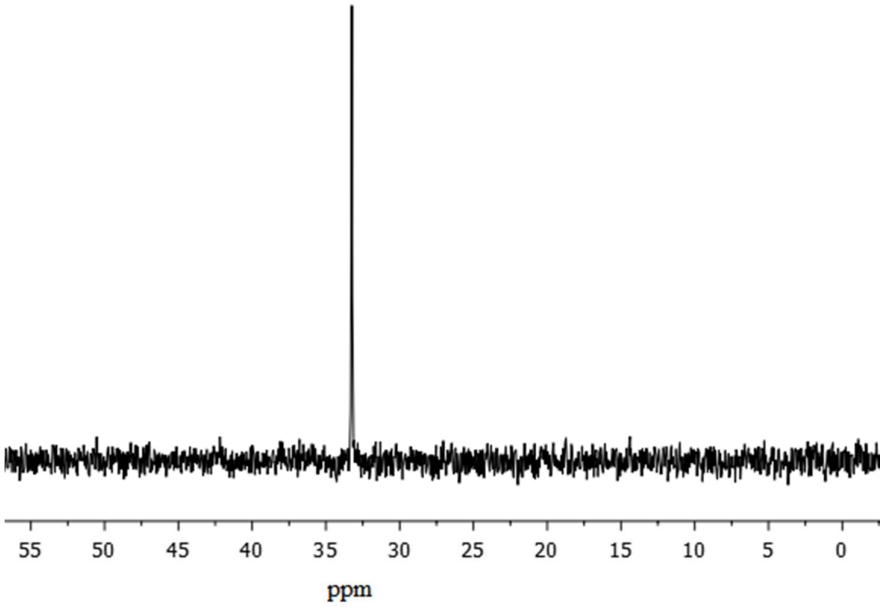

Figure S24. ^{31}P NMR spectrum of $[Au_2(L^5)_2]$.

References

[1] A. Castiñeiras and R. Pedrido, *Dalton Trans.*, 2012, **41**, 1363.

[2] a) A. Castiñeiras and R. Pedrido, *Inorg. Chem.,* 2009, **48**, 4847; b) A. Castiñeiras and R. Pedrido, *Dalton Trans.*, 2010, **39**, 3572.

[3] A. Castiñeiras and R. Pedrido, *Inorg. Chem.,* 2008, **47**, 5534.